horticulturae

MDPI

Article

Expression Analysis and Interaction Protein Screening of CoZTL in *Camellia oleifera* Abel

Shuangshuang Ren [1,2,3,4], Lemei Juan [1,2,3,4], Jiacheng He [1,2,3,4], Qian Liu [1,2,3,4], Jindong Yan [1,2,3,4,*] and Jian'an Li [1,2,3,4,*]

1 Key Laboratory of Cultivation and Protection for Non-Wood Forest Trees of Ministry of Education, Central South University of Forestry and Technology, Changsha 410004, China
2 Key Laboratory of Non-Wood Forest Products of Forestry Ministry, Central South University of Forestry and Technology, Changsha 410004, China
3 Yuelu Mountain Laboratory Non-Wood Forests Variety Innovation Center, Changsha 410004, China
4 Key Laboratory of Breeding and Cultivation of Non-Wood Forest, National Forestry and Grassland Administration, Changsha 410004, China
* Correspondence: yjd0731@outlook.com (J.Y.); lja0731@1126.com (J.L.)

Abstract: *Camellia oleifera* Abel., which produces fruits of high comprehensive utilization value, is an important woody oil tree in China. ZEITLUPE (ZTL) is a blue light receptor and clock component protein that is involved in various physiological and biochemical processes. However, the expression pattern and function of *C. oleifera* ZTL (CoZTL) remain unclear. In this study, the coding sequence of the *CoZTL* gene was isolated and the protein function was explored using bioinformatics and expression analyses and heterologous expression techniques. The results showed that the CoZTL protein was highly conserved during evolution and was on the same branch of the evolutionary tree as the ZTL proteins from *Ipomoea nil* and *Nicotiana attenuata*. *CoZTL* was mainly expressed in the fruit shells and stems of *C. oleifera*, and its expression level fluctuated greatly during flower bud development. Transgenic *CoZTL*-overexpressing *Arabidopsis* plants showed delayed flowering under long-day conditions as well as light-dependent promotion of hypocotyl elongation. Furthermore, yeast two-hybrid library screening revealed that seven *C. oleifera* proteins (CoAAT, Coβ-GAL, CoLAT52-like, CoCAR4-like, CoAO, CoUQCC1, and CoADF 2) interacted with CoZTL. Our results indicate that CoZTL plays an important role in *C. oleifera* flowering and hypocotyl growth.

Keywords: *Camellia oleifera* Abel.; ZEITLUPE; overexpression; flowering; hypocotyl; yeast two-hybrid

check for updates

Citation: Ren, S.; Juan, L.; He, J.; Liu, Q.; Yan, J.; Li, J. Expression Analysis and Interaction Protein Screening of CoZTL in *Camellia oleifera* Abel. *Horticulturae* **2023**, *9*, 833. https://doi.org/10.3390/horticulturae9070833

Academic Editors: Denis V. Yanykin, Alexander S. Voronkov and Jose V. Die

Received: 10 April 2023
Revised: 25 June 2023
Accepted: 18 July 2023
Published: 21 July 2023

Copyright: © 2023 by the authors. Licensee MDPI, Basel, Switzerland. This article is an open access article distributed under the terms and conditions of the Creative Commons Attribution (CC BY) license (https://creativecommons.org/licenses/by/4.0/).

1. Introduction

Camellia oleifera Abel. is a woody oil tree of the family Theaceae [1]. The seeds of this plant can be pressed to release tea oil, which has a long history of consumption in China and is well received by consumers. Studies have shown that tea oil contains up to 90% unsaturated fatty acids and a variety of bioactive substances, such as flavonoids, tocopherols, squalene, and triterpenoids, all of which have both medicinal and edible value [2–4]. For a long time, the phenomenon of more flowers and fewer fruits was common in the production of *C. oleifera*, mainly for two reasons. First, the flowering period occurs in autumn and winter, when the temperature is low and the weather is changeable, which is not conducive to flowering and pollination [5,6]. Second, the self-incompatibility of *C. oleifera* leads to a low fruit-set rate [7]. At present, cross-pollination is used to increase the fruit-set rate to raise the fruit yield of *C. oleifera* [8]. However, bad weather during the flowering period still has an uncontrollable influence on fruit setting and the early development of young fruits. Therefore, it would be beneficial to increase the yield of *C. oleifera* by selecting a variety with a more suitable flowering period.

Light is the main environmental indicator used by plants to detect seasonal and diurnal changes [9]. Various plant photoreceptors can sensitively perceive light signals

and transmit them to the core oscillators of the biological clock, which integrates various external environmental signals for adaptive regulation, the primary way in which plant growth and development are regulated [10–12]. Blue light, which has a wavelength range of 400–500 nm, is involved in the regulation of plant photomorphogenesis, photosynthesis, and the synthesis of active substances [13–15]. Blue light receptors have been shown to be involved not only in these above-mentioned processes but also in the regulation of the plant photoperiod, phototropism, stress response, and organ development [16,17].

Zeitlupe (ZTL) is a blue light receptor and clock component protein that plays a specific role in many biological processes [18]. The protein is mainly made up of light–oxygen–voltage (LOV) and F-box domains. The LOV domain senses blue light and interacts physically with other proteins [19], whereas the F-box domain serves as a ubiquitin ligase-binding site for formation of the Skp–Cullin–F-box-protein $(SCF)^{ZTL}$ complex, which degrades proteins bound to the LOV domain [20]. Studies have shown that ZTL affects the period of the core oscillator of the circadian clock by degrading timing of CAB expression 1 (TOC1) and pseudo-response regulator (PRR) proteins [21]. Overexpression of the *ZTL* gene in *Arabidopsis thaliana* (*AtZTL*) can lead to circadian rhythm disorder, whereas its deletion results in circadian rhythm shortening. ZTL can indirectly regulate hypocotyl elongation, the shading response, and thermomorphogenesis by degrading TOC1 and PRRs and interacting with phytochromes A/B to maintain an abundance of phytochrome-interacting factors (PIFs) [22]. The transcription level of the CONSTANS (CO) protein and its regulation of *FLOWERING LOCUS T* (*FT*) gene expression are key to the photoperiodic flowering response [23]. AtZTL has also been found to maintain the abundance of CO protein by interacting with the GIGANTEA (GI) protein [24], thus promoting expression of the *CO*/*FT* module and further affecting the flowering time of *A. thaliana*. Additionally, researchers found that *ZTL*-overexpressing plants were more sensitive to abscisic acid (ABA) [25]. PRR5, a known target of ZTL, interacts with the Open Stomata 1 (OST1) protein to regulate the ABA response in *Arabidopsis* and *Poplar* [26], thus linking the circadian clock to ABA regulation. Given that ZTL is a key protein connecting the light, circadian clock, and ABA pathways, exploring its function and interaction network would have reference value in aiding our understanding of the mechanisms behind the coordinated regulation of plant growth and development through different pathways.

In this study, we found that the ZTL protein of *C. oleifera* (CoZTL) delayed the flowering time and promoted hypocotyl elongation in transgenic *Arabidopsis* lines. The expression pattern of *CoZTL* in *C. oleifera* revealed that the gene was relatively highly expressed in fruit shells and stems simultaneously, whereas its expression was significantly changed at different flower bud stages. Yeast two-hybrid library screening identified seven *C. oleifera* proteins that interacted with CoZTL; namely, aspartate aminotransferase_cytoplasmic (CoAAT), beta-glactosidase (Coβ-GAL), CoLAT52-like, C2-DOMAIN ABA-RELATED 4-like (CoCAR4-like), L-ascorbate oxidase (CoAO), ubiquinol-cytochrome-c reductase complex assembly factor 1 (CoUQCC1), and actin-depolymerizing factor 2 (CoADF2). These results provide a reference for understanding the biological role of ZTL in *C. oleifera* as well as the flowering mechanism of the plant.

2. Materials and Methods

2.1. Plant Materials and Growth Conditions

The 5-year-old *C. oleifera* 'Huashuo' trees were planted in Central South University of Forestry and Technology (112.994587° E, 28.131841° N), *Arabidopsis* plants were planted in the greenhouse (light 16 h, dark 8 h, 22 °C), seeds of transgenic *Arabidopsis* needed to be disinfected and sown on 1/2 MS (50 mg/L Kanamycin) solid medium plates for screening, after vernalizing in the dark at 4 °C for 2 d, the plates were transferred to the greenhouse for two weeks, and then the seedlings were transplanted to perlite/nutrient soil mixed substrate for further cultivation.

2.2. RNA, DNA Extraction and cDNA Synthesis

The plant materials were ground into powder by liquid nitrogen, and the total RNA of *C. oleifera* and *Arabidopsis* was extracted by using EZ-10 DNA Away RNA mini-preps kit (BBI, Shanghai, China), and the genomic DNA of *Arabidopsis* was extracted by Super Plant Genomic DNA Kit (Polychardes & Polychromatics-Rich) (Tiangen, Beijing, China) and cDNA synthesis used HISCRIPT II 1st strand cDNA Synthesis Kit (+GDNA Wiper) (Vazyme, Nanjing, China).

2.3. CDS Isolation and Vector Construction of CoZTL

The CDS sequence of *CoZTL* was isolated from the cDNA of *C. oleifera* leaves and cloned into the pCAMBIA2300 overexpression vector to produce the recombinant plasmid p2300-35S-*CoZTL*. The *CoZTL* specific primers (Table A1) were designed in Primer Premier 5, and the PCR amplification reaction was performed using Phantamax Super-Fidelity DNA Polymerase (Vazyme, Nanjing, China), the reaction condition is shown in Table A2, then PCR product was detected with 1% agarose. It was ligated to a pCAMBIA2300 vector which was linearized by FastDigest BamHI (Thermo Fisher, Shanghai, China), and the recombinant plasmid was transformed into *E. coli* DH5α and sequenced. (Tsingke, Beijing, China).

2.4. Bioinformatics Analysis of CoZTL

The sequencing results were compared with the CDS sequence of *CoZTL* using DNAMAN software and translated nucleic acid sequences into protein sequences on the online website (https://www.lynnon.com/, accessed on 8 November 2022). The Expasy (https://www.expasy.org/, accessed on 8 November 2022) and DeepTMHMM (https://dtu.biolib.com/DeepTMHMM, accessed on 8 November 2022) were used to analyze the physicochemical properties of CoZTL protein, the conserved domains and motifs search were acquired from NCBI (https://www.ncbi.nlm.nih.gov/, accessed on 20 February 2023) and MEME (https://meme-suite.org/meme/index.html, accessed on 21 March 2023), the NCBI was also used for blastp search of ZTL protein sequences, which were subjected to multiple alignments and phylogenetic tree construction in DNAMAN and MEGA 11, the phylogenetic tree was constructed by Maximum Likelihood [27].

2.5. Expression Analysis of CoZTL in C. oleifera

The flower buds of *C. oleifera* were collected every 15 d from 31 July until 30 October [28]. The roots, stems, leaves, flowers, and fruits of *C. oleifera* were collected at same time in mid-September. These materials were put into liquid nitrogen and stored at −80 °C for extracting total RNA and cDNA synthesis, the expression level of *CoZTL* was determined by qRT-PCR experiments using ChamQ Universal SYBR qPCRMaster MixRT-qPCR (Vazyme, Nanjing, China), the internal reference gene was *CoGAPDH* [29]. The qRT-PCR primers are shown in Table A1, and the reaction conditions are shown in Table A3. The qRT-PCRs were performed on the CFX96 real-time PCR system (Bio-Rad, California, USA). Each reaction was performed with three technical replicates. The calculation method for qRT-PCR was $2^{-\Delta\Delta CT}$.

2.6. Transformation and Identification of Arabidopsis

The recombinant plasmid was transformed into *Agrobacterium tumefaciens* AGL0 by electroporation, then transformed Col-0 plants using the floral dip method [30]. The transformed T0 seeds were harvested and sowed on 1/2 MS (50 mg/L Kana) solid medium for screening. After two weeks of cultivation, the T0 seeding with four leaves and long roots on the plate were selected, then transferred them to pots for cultivation. When the plants had about 10 leaves, we collected the leaves of each Col-0 and T0 generation *Arabidopsis* plants to extract RNA and DNA. The transgenic *Arabidopsis* lines were identified by PCR and qRT-PCR, the internal reference gene was *AtACTIN2* [31], the primers are shown in Table A1.

2.7. Phenotypic Observation of Transgenic Arabidopsis

The transgenic *Arabidopsis* plants were repeatedly screened for the T2 generation, and the T2 seeds were used for phenotypic observation. We analyzed the phenotypic data using SPSS's ANOVA and Tukey's HSD (Honest Significant Difference) test tool.

2.7.1. Flowering Observation

After the seeds of *Arabidopsis* were disinfected, col-0 was sprinkled on the solid medium, the seeds of Col-0 and *ztl* (SALK_035701) were sown on 1/2 MS solid medium plates, the T2 generation transgenic *Arabidopsis* seeds were sown on 1/2 MS (50 mg/L Kana) solid medium plates, after vernalization at 4 °C for 2 d, the plates were transferred to the greenhouse at 22 °C for 16 h/8 h (light/dark) for two weeks, then transplanted 15 seedlings of each *Arabidopsis* line into pots and cultivated at 22 °C, 16 h/8 h (light/dark), we recorded the bolting time and number of rosette leaves at the time of bolting.

2.7.2. Hypocotyl Observation

After disinfecting of Col-0, *ztl* and T2 generation transgenic *Arabidopsis* seeds, they were sown on the same 1/2 MS solid medium plate, which needed two plates, the plates were vernalized at 4 °C for 4 d. Then placed in a 5000 xl incubator at 22 °C, 16 h/8 h (light/dark) for 1 d; after wrapping one of the plates in tinfoil, the culture was continued for 6 d. Finally, each *Arabidopsis* strain was measured the hypocotyl length of 20 seedlings.

2.8. The Autoactivation Activity Test of CoZTL

The *CoZTL* fragment was cloned into the pGBKT7 vector (the primers are shown in Table A1), and the recombinant plasmid was named *CoZTL*-BD. the experimental group CoZTL-BD+pGADT7, the positive control group pGBKT7-53+pGADT7-T, the negative control group pGBKT7-Lam+pGADT7-T and the blank control group pGBKT7+pGADT7 were transformed into yeast AH109. the yeast colony of each group was selected and resuspended with 50 µL sterile water, then transferred 2.5 µL to SD/-Trp/-Leu/-His (TDO) solid plates with 3-AT gradient settings of 0, 2.5, 5, 10, 15, 20, 30, 40, 50, and 60 mM/L. After the plates were dried, sealed and cultured upside down for 4 d, the lowest 3-AT concentration corresponding to the plate without colony growth was selected for subsequent library screening.

2.9. Screen of Yeast Two-Hybrid Library

The mating method was used for yeast two-hybrid screening, protein-protein interactions could be screened with different selected media [32,33]. First, *CoZTL*-BD was transformed into the yeast AH109, and the yeast colony was picked out into 50 mL of SD/-Trp liquid culture medium and cultured at 30 °C, 200 rpm until the OD_{600} was about 0.8. Then, the yeast cells were collected at the speed of 3000 rpm for 5 min, and the precipitated yeasts were resuspended with 5 mL of SD/-Trp liquid medium to make the cell concentration greater than 1×10^8/mL, and mixed with 1 mL Y187 library yeast. The mixture and 45 mL of 2 YPDA liquid medium were added into a sterile 2 L triangular flask and cultured at 30 °C, 40 rpm for about 16 to 20 h until the appearance of heterozygotes in the shape of "clover" under a microscope. Finally, the yeast cells were collected again at 3000 rpm for 10 min, and resuspended with 5 mL sterile water. The resuspended solution was coated on TDO solid plates with 3-AT about 200 µL/plate, and cultured for 4–6 days. We selected all yeast colonies resuspended in 20 µL sterile water and transferred 2.5 µL of the resuspension to TDO and SD/-Trp/-Leu-His-Ade (QDO) + X-α-Gal plates with 3-AT. Blue yeast colonies were selected and cultured overnight in 5 mL SD/-Trp-leu medium at 30 °C and 200 rpm. Rapid yeast plasmid was used the yeast plasmid was extracted using Quick Yeast Plasmid Preps Kit and transformed into *E. coli* DH5α to sequence. the yeast plasmid was extracted using Quick Yeast Plasmid Preps Kit and transformed into *E. coli* DH5α to sequence.

After the sequencing results were translated into protein sequences, they were analyzed using NCBI blastp tool, and the results were collated. After the plasmids corresponding to each fragment were extracted from *E. coli* DH5α, they were transformed into yeast AH109 with *CoZTL*-BD and verified on TDO and QDO+X-α-gal plates with 3-AT.

3. Results

3.1. Cloning of the CoZTL Coding Sequence and Analysis of the Protein

We isolated the CDS of *ZTL* from the cDNA of *C. oleifera* 'Huashuo' (Figure 1a). The sequence was 1827 bp in length and encoded 609 amino acids. The CoZTL protein, the molecular formula of which was predicted to be $C_{2947}H_{4616}N_{826}O_{872}S_{27}$, had a relative molecular weight of 66.44 kDa, a theoretical pI of 5.78, and an instability index of 41.02 (indicating it is an unstable protein). The aliphatic index of the protein was 88.31, and the average hydrophilicity was −0.104, which was consistent with the ProtScale analysis. The ProtParam tool predicted CoZTL to be an intracellular protein, as it did not contain a transmembrane region. The conserved domain search identified two domains: Per–ARNT–Sim (PAS) and F-box.

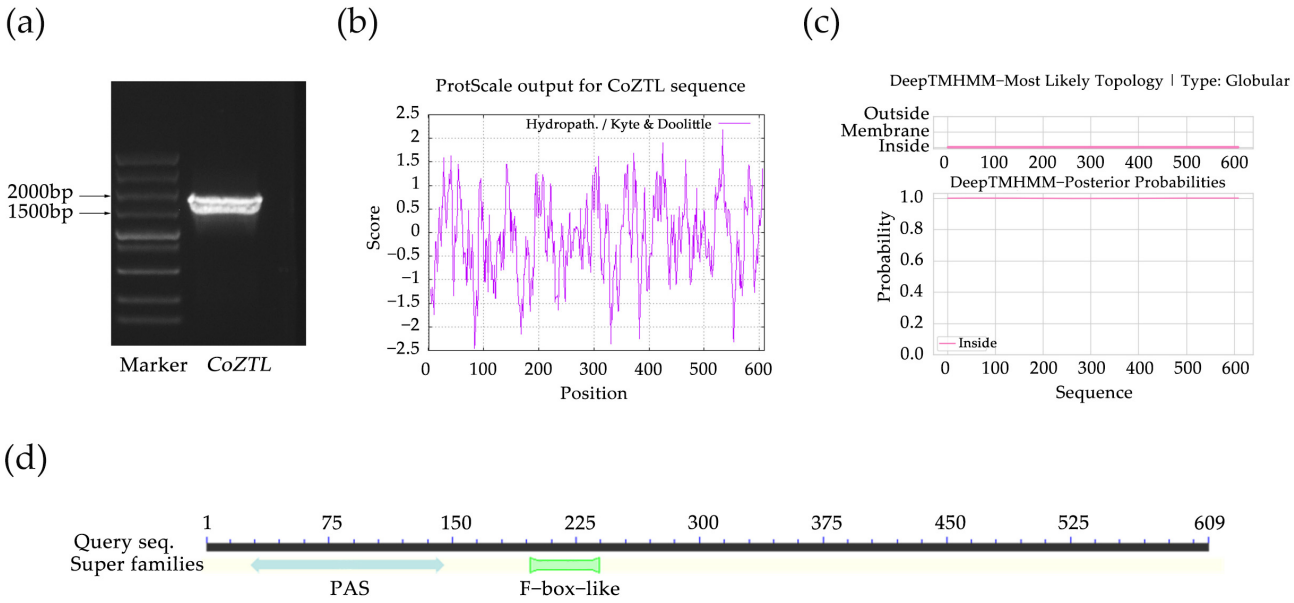

Figure 1. CDS fragment detection and bioinformatics analysis of CoZTL protein Notes: (**a**) CDS fragment detection of *CoZTL* gene. (**b**) Hydrophobicity analysis of CoZTL protein, negative number is hydrophilic, positive number is hydrophobic. (**c**) Transmembrane analysis of CoZTL protein. (**d**) Conserved domains of CoZTL protein.

3.2. Phylogenetic Analysis of CoZTL

We compared the CoZTL protein sequence with the ZTL protein sequences of *A. thaliana*, *Picea abies*, *Triticum aestivum*, *Dimocarpus longan*, and *Glycine max*. As shown in Figure 2a, the lengths of the sequences from the different species were similar. The degree of sequence composition similarity between *C. oleifera* and the five species was 82.98%, 79.39%, 71.82%, 89.82%, and 88.46%, respectively, with the differences being mainly from the N-terminal sequence to the PAS domain and from the PAS domain to the F-box domain. The other regions were highly conserved, which was consistent with the motif analysis results. The motifs of CoZTL and 24 ZTL family members were analyzed, and a phylogenetic tree was constructed (Figure 2b). The tree revealed that CoZTL belonged in the same branch as its counterparts from *Ipomoea nil* (InZTL) and *Nicotiana attenuata* (NaZTL). It was also in the same branch as LOV kelch protein 2 (LKP2) of *Brassica rapa* and *A. thaliana*, indicating that the CoZTL protein might be related to LKP2. Additionally, motif analysis revealed that the

ZTL family of proteins shared more conserved regions. We hypothesize that CoZTL has been highly conserved during evolution.

(a)

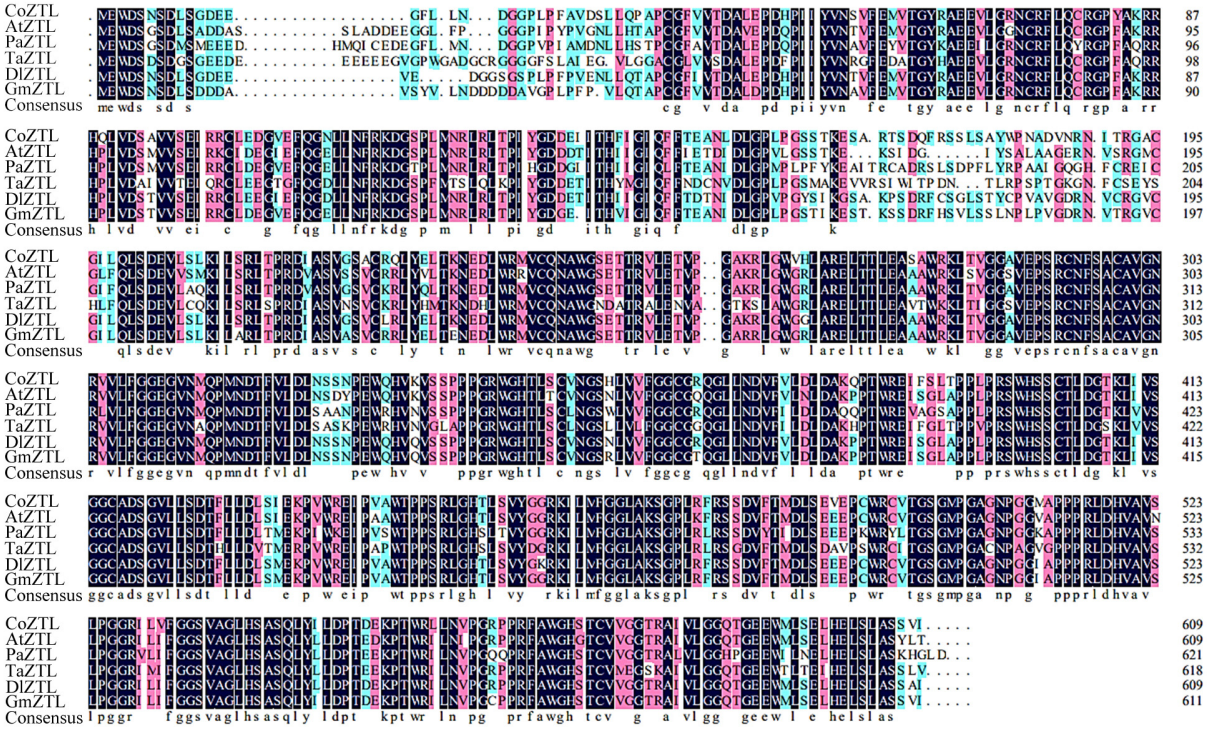

(b)

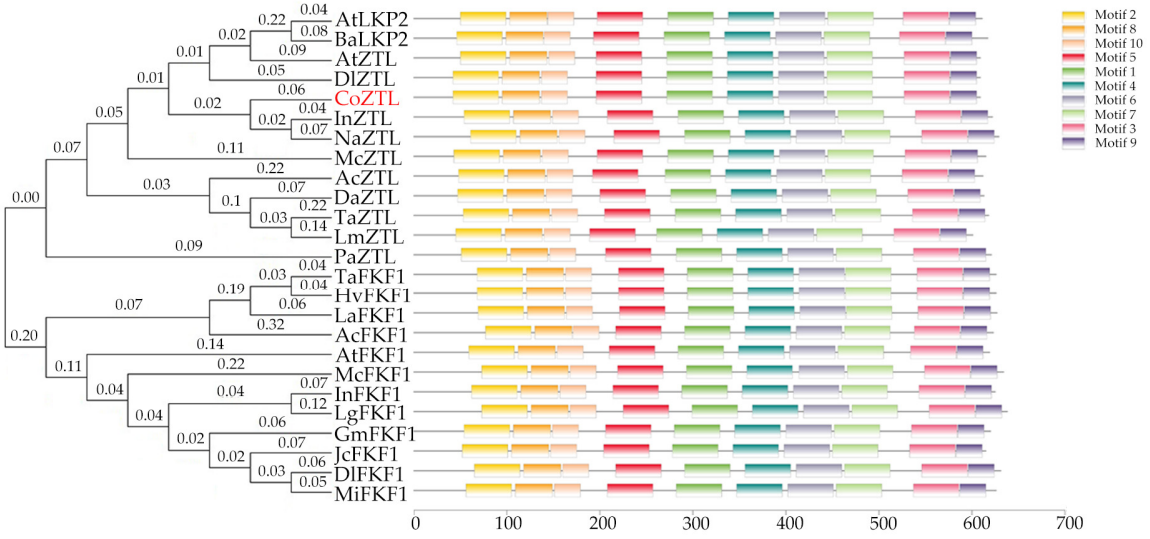

Figure 2. Multiple sequence alignment and phylogenetic tree. Notes: (**a**) Multiple sequence alignment, the ZTL protein sequences are from *A. thaliana*, *Picea abies*, *Triticum aestivum*, *Dimocarpus longan*, and *Glycine max*. Highlight homology level: ■ = 100%, ■ ≥ 75%, ■ ≥ 50%. (**b**) Phylogenetic tree and motifs of ZEITLUPE protein family from *C. oleifera* and other species. The information of 24 protein sequences is shown in Table A4.

3.3. Pattern of CoZTL Expression in C. oleifera

C. oleifera is a type of tree that bears flowers and fruits at the same time. Therefore, the roots, stems, leaves, flower buds, and fruits can be collected at one time, and the fruit shells and seeds can be separated to detect their *CoZTL* expression levels. As indicated in Figure 3a, the gene expression levels were the highest in the stems and fruit shells and the lowest in the roots. Additionally, flower buds from seven stages were collected every 15 d for *CoZTL* expression analysis. The results (Figure 3b) showed that the level of *CoZTL* expression changed significantly during development of the flower buds and peaked in mid-September.

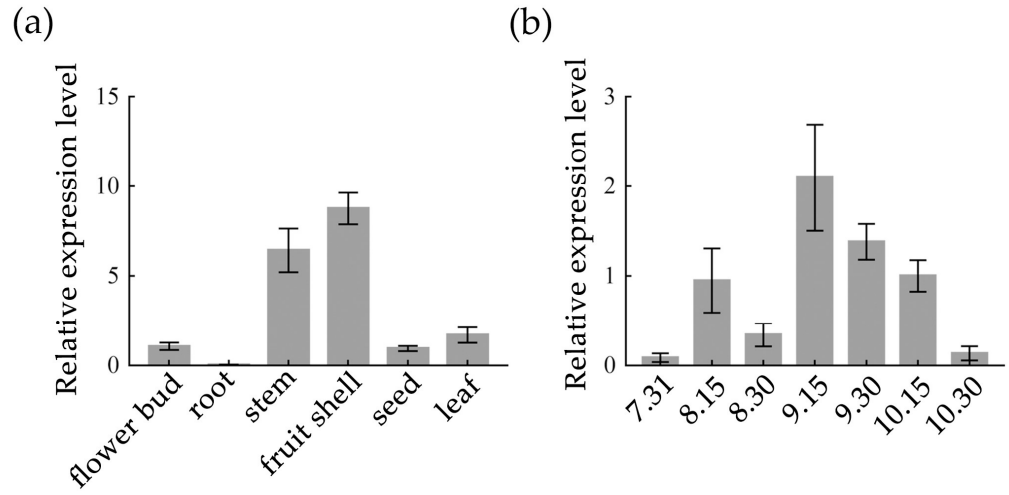

Figure 3. Relative expression level of *CoZTL* in *C. oleifera*. Notes: (**a**) Relative expression level of *CoZTL* in different tissues; (**b**) Relative expression level of *CoZTL* in different stage flower buds. Data are means ± SE.

3.4. Heterologous Overexpression of CoZTL in Arabidopsis

We identified transgenic *Arabidopsis* plants using PCR and qRT-PCR and selected three transgenic lines with different *CoZTL* expression levels (designated 35S-*CoZTL*-1, 35S-*CoZTL*-2, and 35S-*CoZTL*-3) for subsequent phenotype observation (Figure 4a,b). We statistically analyzed the bolting time and number of rosette leaves during bolting of the Col-0 strain, the *ztl* mutant strain, and the three transgenic *Arabidopsis* lines (Figure 4c–e). Compared with Col-0, the three transgenic lines showed delayed bolting and had a significantly higher number of rosette leaves. By contrast, there was no difference in number of rosette leaves between the *ztl* mutant and Col-0 strains. Therefore, we suggest that *CoZTL* overexpression delays flowering in *A. thaliana*.

After vernalization, the seeds of Col-0, the *ztl* mutant, and the three transgenic *Arabidopsis* lines were exposed to light for 1 d to ensure seed germination. After 1 d, the plates were placed in the dark and under weak light conditions. After 6 d, the hypocotyl lengths of each line under the two conditions were measured (Figure 4f–h). Under the dark condition, no significant differences were observed among the groups except for the *ztl* mutant, 35S-*CoZTL*-1, and 35S-*CoZTL*-2. However, under the weak light condition, the hypocotyl length of the three transgenic lines was significantly longer than that of Col-0, whereas that of the *ztl* mutant was significantly shorter. Additionally, the hypocotyl length of 35S-*CoZTL*-2 was significantly longer than that of 35S-*CoZTL*-1. Therefore, we suggest that *CoZTL* overexpression promotes hypocotyl growth in transgenic *Arabidopsis plants*, an effect that requires light conditions.

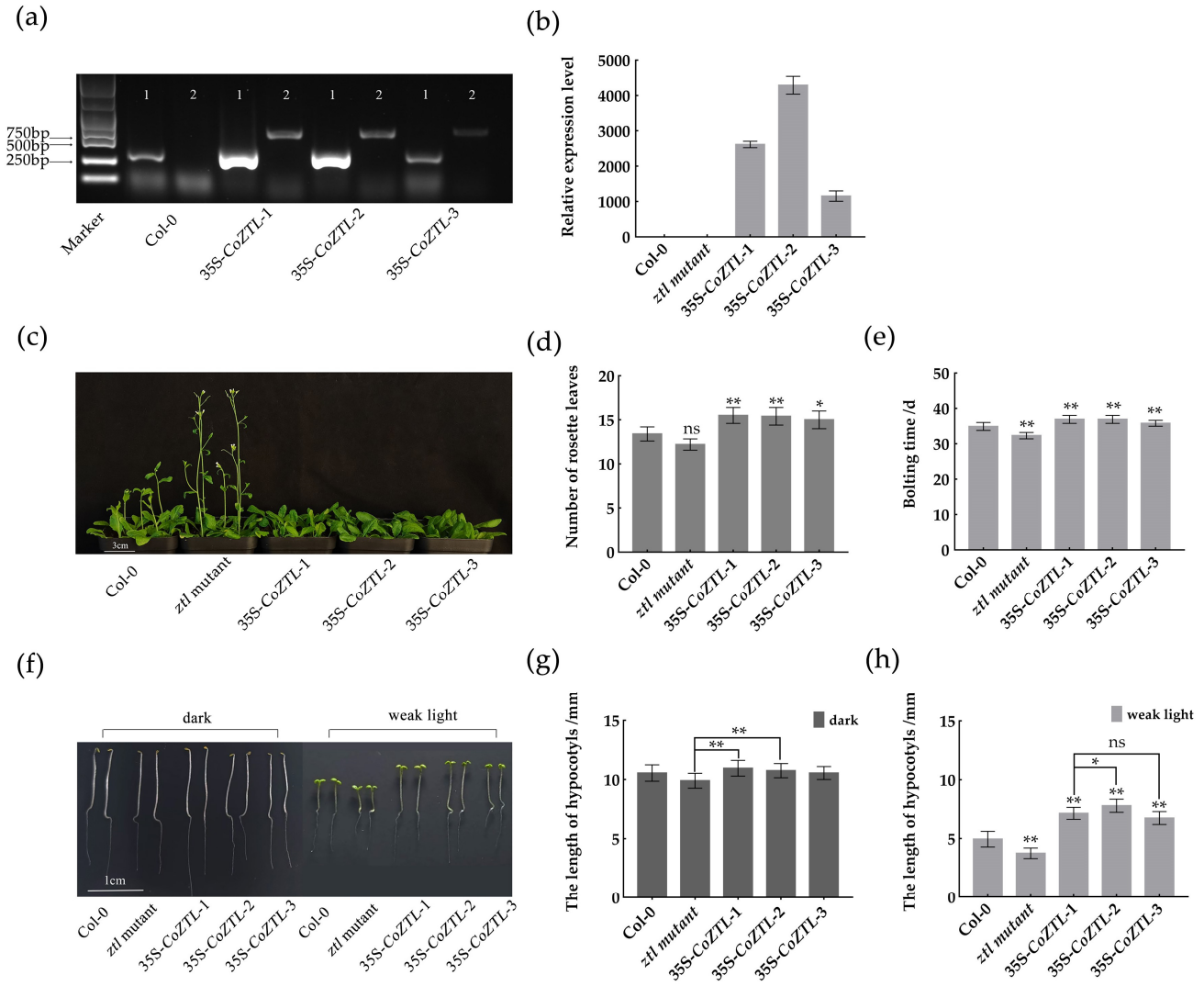

Figure 4. Identification and phenotypic observation of transgenic *Arabidopsis*. Notes: (**a**) Identification of transgenic *Arabidopsis* plants by PCR, the 1 was *AtACTIN2* and 2 was *CoZTL* in picture. (**b**) *CoZTL* gene relative expression levels in *Arabidopsis* plants. Data are means±SE. (**c**) Flowering observation. (**d**) Leaves number at bolting time. (**e**) Bolting time. (**f**) Hypocotyl observation. (**g**) Hypocotyl length under dark. (**h**) Hypocotyl length under weak light. the data are means ± SD. *p*-values were determined using Tukey's HSD test. ns, no statistically significant difference; * $p < 0.05$; ** $p < 0.01$.

3.5. Autoactivation Activity Test and Yeast Two-Hybrid Screening of CoZTL

CoZTL displayed autoactivation activity (Figure 5a), which could be inhibited by the addition of 20 mM 3-AT. Through yeast two-hybrid library screening, we obtained 64 yeast strains for sequencing, which yielded 19 gene fragments. We translated these 19 fragments and searched them using the BLASTP tool. Then, we extracted 10 plasmids corresponding to 10 known protein sequences from *E. coli* DH5α and transferred them into yeast strain AH109 with CoZTL-BD. Only seven protein sequences interacted with CoZTL (Figure 5b). The protein information is shown in Table 1.

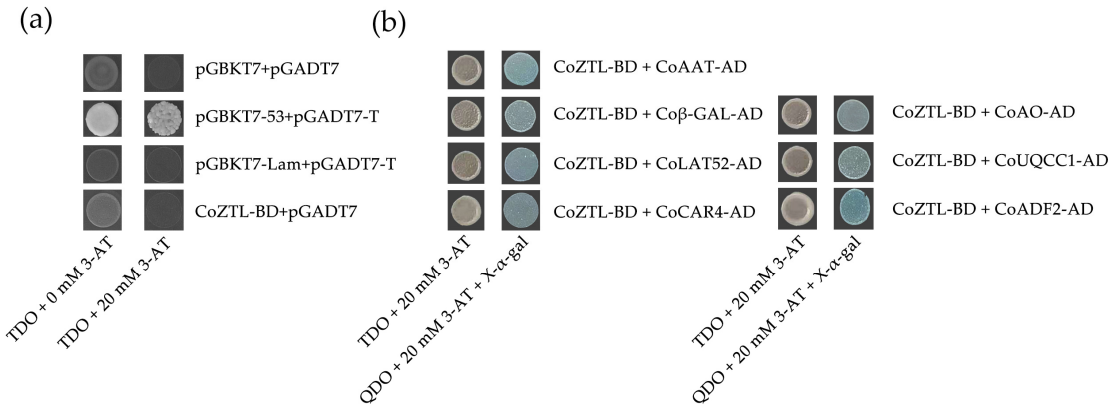

Figure 5. Autoactivation activity test and yeast two-hybrid screening of CoZTL. Notes: (**a**) Detection of autoactivation activity of CoZTL protein (**b**) Validation of interaction between seven proteins and CoZTL.

Table 1. 7 List of proteins that interact with CoZTL protein.

Number	Accession	Protein Name	Short Name
1	XP_028124809.1	aspartate aminotransferase_cytoplasmic	AAT
2	TEA033138	beta-galactosidase	β-GAL
3	XP_028059082.1	anther-specific protein LAT52-like	LAT52-like
4	XP_028059865.1	C2-DOMAIN ABA-RELATED 4-like	CAR4-like
5	XP_028126352.1	L-ascorbate oxidase	AO
6	XP_028108523.1	ubiquinol-cytochrome-c reductase complex assembly factor 1	UQCC1
7	XP_028082200.1	actin-depolymerizing factor 2	ADF2

4. Discussion

In this study, we isolated the CDS of *CoZTL* and performed translation and bioinformatics analyses of its encoded protein. We found that CoZTL was an intracellular protein, and its primary structure contained PAS and F-box domains. The CoZTL protein sequence was highly conserved, exhibiting more than 70% similarity with ZTLs from other species. These results are consistent with the ZTL protein characteristics reported for other species [34,35].

Additionally, the phylogenetic tree revealed that CoZTL belonged to the same branch as InZTL and NaZTL, which are more closely related to each other. These findings provide a reference for studying the function of CoZTL during the development of *C. oleifera*. Although previous studies have shown that ZTL is a blue light receptor, its expression is not affected by light. The expression of *InZTL* in *Ipomoea nil* was higher in the cotyledons and sepals and lowest in the roots [36], whereas the expression of *AtZTL* in *A. thaliana* was also lowest in the roots. These results were different from ours, where *CoZTL* expression was highest in the fruit shells and lowest in the roots of *C. oleifera*. We also found that the *CoZTL* expression level changed dynamically during the development of flower buds, which was consistent with the results of rice and soybean studies in which the expression patterns of *OsZTL* and *GmZTL* also changed at different plant development stages [37–39]. Researchers also found that *GmZTL3* mRNA in soybean was accumulated in various leaves and concentrated in mature seeds before flowering [40], which was similar to our finding of a relatively high level of *CoZTL* expression in the fruits of *C. oleifera* before flowering. At present, not many studies that have reported relative expression levels have described the developmental stages of the plants, and the common points of *ZTL* expression patterns are not clear. Therefore, we speculate that the reason for the changes in the *CoZTL* expression pattern may be related to the degree of organ development at different periods.

Changes in the circadian rhythm often lead to abnormal hypocotyl growth and flowering time [41]. The abundance of ZTL—a clock protein—is controlled by the biological clock, and its expression depends on protease degradation. It is generally assumed that *ZTL*

overexpression regulates the level of *CO* gene transcription and reduces the inhibition of phytochrome-interacting factors by phytochromes A/B, which leads to delayed flowering and promotes hypocotyl elongation [42,43]. These observations are consistent with the results of this study, in which transgenic *CoZTL*-overexpressing *Arabidopsis* plants showed delayed flowering under long-day conditions as well as light-dependent promotion of hypocotyl elongation.

As a blue light receptor protein, ZTL may be involved in blue light-regulated photomorphology and biosynthetic pathways, such as hypocotyl elongation, phototropic movement, shade avoidance syndrome, and primary metabolite synthesis. However, the functions and regulatory control mechanisms of ZTL in these pathways remain unclear. In this study, yeast two-hybrid library screening identified seven protein sequences that interacted with CoZTL. One of those proteins, CAR4-like, binds to and recruits ABA receptors in response to high concentrations of Ca^{2+} on the cell membrane [44–46]. *CAR1*-overexpressing *A. thaliana* plants were demonstrated to be more sensitive to ABA-mediated seedling and bud growth inhibition than their wild-type counterparts, whereas *car3* mutant seedlings were less sensitive to the ABA-mediated inhibition of seedling establishment and root growth [45,46], which was opposite to the sensitivity to ABA shown by our *CoZTL*-overexpressing and *ztl* mutant lines of *A. thaliana*. These results provide new insights into the correlation between ZTL and ABA signaling pathways.

CoADF2, the major function of which is to cut off and depolymerize filamentous actin, is directly or indirectly involved in cell division, elongation, and signal transduction [47]. The knockout of *AtADF1* significantly increased the lengths of the hypocotyl, roots, and stem, whereas its overexpression significantly shortened those lengths. Moreover, the flowering time was significantly delayed in plants with downregulated *AtADF1* expression, whereas it was similar between *AtADF1*-overexpressing and wild-type plants. These findings are opposite to the effects of ZTL on hypocotyl elongation and flowering in our study [48,49]. Huang conducted a comprehensive analysis of the promoter structure and expression patterns of 11 ADFs of *Oryza sativa* and found that there were *cis*-acting elements related to stress in the 1 kb promoter region, including ABA response elements, dehydration response elements, and low-temperature response elements [50], but no direct association was found between ADF and ZTL.

CoAAT and Coβ-GAL are enzymes that synthesize amino acids and hydrolyze d-galactosyl residues from polymers, oligosaccharides, or secondary metabolites. They are involved in plant amino acid and sugar metabolism, which is consistent with the role of blue light in regulating the content of free amino acids and soluble sugars in plants [51,52]. AO, which converts ascorbate to monodehydroascorbate and is located in the cell wall, is related to plant growth and development, stress resistance, and senescence [53,54]. The *AO* expression levels in flowers and fruits are high, which is conducive to the induction of flowering and fruit ripening. Although the expression level of *CoZTL* is also high in fruits, its overexpression could delay flowering, and there may be a negative feedback relationship involved in this process. With regard to the anther-specific proteins CoLAT52-like and CoUQCC1, their correlation with ZTL could not be surmised owing to the lack of reports about their functions.

5. Conclusions

In this study, we conducted a comprehensive analysis of the *ZTL* gene in *C. oleifera*. We observed a close relationship between the ZTL protein of *C. oleifera* and the ZTL protein of *Ipomoea nil* by constructing a phylogenetic tree. Meanwhile, we also found that the expression of ZTL gene showed significant changes during the organ development of *C. oleifera*, rice and soybean. In addition, transgenic *CoZTL*-overexpressing *Arabidopsis* plants showed delayed flowering under long-day conditions as well as light-dependent promotion of hypocotyl elongation. Moreover, the yeast two-hybrid experiment results showed that CoZTL protein physically interacted with ABA receptor protein CAR4-like and two proteins (ADF2, AO) which were involved in plant growth and development. Overall, our results enhance our understanding of the *ZTL* gene in *C. oleifera*, while also

providing potential directions for future investigations into the function of the *ZTL* gene in plant growth and development.

Author Contributions: Conceptualization, J.Y. and J.L.; methodology, J.Y. and S.R.; software, S.R.; validation, S.R. and J.Y.; formal analysis, S.R., L.J., J.H. and Q.L.; investigation, S.R., L.J., J.H. and Q.L.; resources, J.Y. and J.L.; data curation, S.R., L.J., J.H. and Q.L.; writing—original draft preparation, S.R.; writing—review and editing, S.R., Q.L. and J.Y.; visualization, J.Y.; supervision, J.Y. and J.L.; project administration, J.Y. and J.L.; funding acquisition, J.Y. and J.L. All authors have read and agreed to the published version of the manuscript.

Funding: This research was funded by China Postdoctoral Science Foundation, grant number 2021M703653, https://jj.chinapostdoctor.org.cn/website/zhengshuchayan.html (accessed on 19 July 2023), Natural Science Foundation of Hunan Province, grant number 2023JJ41041, https://kjt.hunan.gov.cn/kjt/xmxx/xmlx/202305/t20230516_29339472.html (accessed on 19 July 2023), Changsha Natural Science Foundation, grant number kq2202281, http://kjj.changsha.gov.cn/zfxxgk/tzgg_27202/202202/t20220221_10477123.html (accessed on 19 July 2023), and Hunan Forestry Science and Technology Innovation Project, grant number XLK202101-2.

Institutional Review Board Statement: Not applicable.

Informed Consent Statement: Not applicable.

Data Availability Statement: Not applicable.

Conflicts of Interest: The authors declare no conflict of interest.

Appendix A

Table A1. The list of Primer.

Primer Name	Primer Sequence (5′ to 3′)
CoZTL-2300-F	GGTACCCGGGGATCCATGGAGTGGGACAGCAATTC
CoZTL-2300-R	CCTCTAGAGGATCCGATAACAGAACTTGCCAAAGATAG
CoZTL-trans-F	GAAGATGCCTCTGCCGACA
CoZTL-trans-R	TCTTCAAGGCATCTTCTTATTTCTG
CoZTL-qPCR-F	ATTCTGATCTGAGCGGCGAC
CoZTL-qPCR-R	TTCCGCCCAAGAACCTCTTC
GAPDH-F	CTACTGGAGTTTTCACCGA
GAPDH-R	TAAGACCCTCAACAATGCC
ACTIN-F	CACTGTGCCAATCTACGAGGGT
ACTIN-R	CACAAACGAGGGCTGGAACAAG
CoZTL-BD-F	AATTCCCGGGGATCCATGGAGTGGGACAGCAATTC
CoZTL-BD-R	CAGGTCGACGGATCCGATAACAGAACTTGCCAAAGATAG

Table A2. The reaction condition of PCR.

Step	Temperature/°C	Time	Cycles
Predenaturation	95 °C	3 min	35
Denaturation	95 °C	15 s	
Annealing	58 °C	15 s	
Extension	72 °C	2 min	
Complete extension	72 °C	5 min	
Finish	22 °C	forever	

Table A3. The reaction condition of qRT-PCR.

Step	Temperature/°C	Time	Cycles
Predenaturation	95 °C	5 min	45
Denaturation	95 °C	30 s	
Annealing	58 °C	30 s	
Extension	72 °C	30 s	

Table A4. The information of 24 proteins.

Protein	Accession	Species	Protein	Accession	Species
AtLKP2	NP_849983.1	*Arabidopsis thaliana*	AcZTL	ACT22763.1	*Allium cepa*
AtFKF1	AAF32298.2		AcFKF1	ACT22762.1	
AtZTL	OAO90691.1		TaZTL	ABR14627.1	*Triticum aestivum*
DlZTL	AHZ89710.1	*Dimocarpus longan*	TaFKF1	ABL11478.1	
DlFKF1	AHZ89704.1		GmFKF1	NP_001235886.2	*Glycine max*
InZTL	ABC25060.2	*Ipomoea nil*	MiFKF1	UDP61404.1	*Mangifera indica*
InFKF1	AIZ66163.1		JcFKF1	AXF53797.1	*Jatropha curcas*
NaZTL	AFA35963.1	*Nicotiana attenuata*	HvFKF1	KAE8795993.1	*Hordeum vulgare*
McZTL	AAQ73527.1	*Mesembryanthemum crystallinum*	PaZTL	AGH20050.1	*Picea abies*
McFKF1	AAQ73528.1		LgFKF1	UDM54773.1	*Luculia gratissima*
BaLKP2	AIC37536.1	*Brassica rapa*	LmZTL	BDI21198.1	*Lemna minor*
LaFKF1	QTZ25449.1	*Lolium arundinaceum*	DaZTL	KAH7671732.1	*Dioscorea alata*

References

1. Chen, T.; Liu, L.; Zhou, Y.L.; Zheng, Q.; Luo, S.Y.; Xiang, T.T.; Zhou, L.J.; Feng, S.L.; Yang, H.Y.; Ding, C.B. Characterization and comprehensive evaluation of phenotypic characters in wild *Camellia oleifera* germplasm for conservation and breeding. *Front. Plant Sci.* **2023**, *14*, 1052890. [CrossRef]
2. Ma, J.L.; Ye, H.; Rui, Y.K.; Chen, G.C.; Zhang, N.Y. Fatty acid composition of *Camellia oleifera* oil. *J. Verbr. Lebensm.* **2011**, *6*, 9–12. [CrossRef]
3. Quan, W.X.; Wang, A.P.; Gao, C.; Li, C.C. Applications of Chinese *Camellia oleifera* and its By-Products: A Review. *Front. Chem.* **2022**, *10*, 921246. [CrossRef]
4. Luan, F.; Zeng, J.S.; Yang, Y.; He, X.R.; Wang, B.J.; Gao, Y.B.; Zeng, N. Recent advances in *Camellia oleifera* Abel: A review of nutritional constituents, biofunctional properties, and potential industrial applications. *J. Funct. Foods* **2020**, *75*, 104242. [CrossRef]
5. Wu, L.L.; Li, J.A.; Gu, Y.Y.; Zhang, F.H.; Gu, L.; Tan, X.F.; Shi, M.W. Effect of Chilling Temperature on Chlorophyll Florescence, Leaf Anatomical Structure, and Physiological and Biochemical Characteristics of Two *Camellia oleifera* Cultivars. *Int. J. Agric. Biol.* **2020**, *23*, 777–785.
6. Zhang, Y.Q.; Guo, Q.Q.; Luo, S.Q.; Pan, J.W.; Yao, S.; Gao, C.; Guo, Y.Y.; Wang, G. Light Regimes Regulate Leaf and Twigs Traits of *Camellia oleifera* (Abel.) in *Pinus massoniana* Plantation Understory. *Forests* **2022**, *13*, 918. [CrossRef]
7. He, Y.F.; Song, Q.Q.; Chen, S.P.; Wu, Y.F.; Zheng, G.H.; Feng, J.L.; Yang, Z.J.; Lin, W.J.; Li, Y.; Chen, H. Transcriptome analysis of self- and cross-pollinated pistils revealing candidate unigenes of self-incompatibility in *Camellia oleifera*. *J. Hortic. Sci. Biotechnol.* **2020**, *95*, 19–31. [CrossRef]
8. Hu, G.X.; Gao, C.; Fan, X.M.; Gong, W.F.; Yuan, D.Y. Pollination Compatibility and Xenia in *Camellia oleifera*. *Hortscience* **2020**, *55*, 898–905. [CrossRef]
9. Panchy, N.; von Arnim, A.G.; Hong, T. Early Detection of Daylengths with a Feedforward Circuit Coregulated by Circadian and Diurnal Cycles. *Biophys. J.* **2020**, *119*, 1878–1895. [CrossRef]
10. Kong, S.G.; Okajima, K. Diverse photoreceptors and light responses in plants. *J. Plant Res.* **2016**, *129*, 111–114. [CrossRef]
11. Mawphlang, O.I.L.; Kharshiing, E.V. Photoreceptor Mediated Plant Growth Responses: Implications for Photoreceptor Engineering toward Improved Performance in Crops. *Front. Plant Sci.* **2017**, *8*, 1181. [CrossRef]
12. Voitsekhovskaja, O.V. Phytochromes and Other (Photo)Receptors of Information in Plants. *Russ. J. Plant Physiol.* **2019**, *66*, 351–364. [CrossRef]
13. Abidi, F.; Girault, T.; Douillet, O.; Guillemain, G.; Sintes, G.; Laffaire, M.; Ben Ahmed, H.; Smiti, S.; Huche-Thelier, L.; Leduc, N. Blue light effects on rose photosynthesis and photomorphogenesis. *Plant Biol.* **2013**, *15*, 67–74. [CrossRef]
14. Fraszczak, B. The Effect of Different Doses of Blue Light on the Biometric Traits and Photosynthesis of Dill Plants. *Not. Bot. Horti Agrobot. Cluj-Napoca* **2016**, *44*, 34–40. [CrossRef]
15. Liang, Y.; Kang, C.Q.; Kaiser, E.; Kuang, Y.; Yang, Q.C.; Li, T. Red/blue light ratios induce morphology and physiology alterations differently in cucumber and tomato. *Sci. Hortic.* **2021**, *281*, 109995. [CrossRef]
16. Christie, J.M.; Blackwood, L.; Petersen, J.; Sullivan, S. Plant Flavoprotein Photoreceptors. *Plant Cell Physiol.* **2015**, *56*, 401–413. [CrossRef]
17. Lehmann, P.; Nothen, J.; von Braun, S.S.; Bohnsack, M.T.; Mirus, O.; Schleiff, E. Transitions of gene expression induced by short-term blue light. *Plant Biol.* **2011**, *13*, 349–361. [CrossRef]

18. Pudasaini, A.; Zoltowski, B.D. Zeitlupe Senses Blue-Light Fluence to Mediate Circadian Timing in Arabidopsis thaliana. *Biochemistry* **2013**, *52*, 7150–7158. [CrossRef]
19. Demarsy, E.; Fankhauser, C. Higher plants use LOV to perceive blue light. *Curr. Opin. Plant Biol.* **2009**, *12*, 69–74. [CrossRef]
20. Ito, S.; Song, Y.H.; Imaizumi, T. LOV Domain-Containing F-Box Proteins: Light-Dependent Protein Degradation Modules in Arabidopsis. *Mol. Plant* **2012**, *5*, 573–582. [CrossRef]
21. Seo, D.; Park, J.; Park, J.; Hwang, G.; Seo, P.J.; Oh, E. ZTL regulates thermomorphogenesis through TOC1 and PRR5. *Plant Cell Environ.* **2023**, *46*, 1442–1452. [CrossRef] [PubMed]
22. Zou, Y.; Li, R.; Baldwin, I.T. ZEITLUPE is required for shade avoidance in the wild tobacco Nicotiana attenuata. *J. Integr. Plant Biol.* **2020**, *62*, 1341–1351. [CrossRef] [PubMed]
23. Takase, T.; Nishiyama, Y.; Tanihigashi, H.; Ogura, Y.; Miyazaki, Y.; Yamada, Y.; Kiyosue, T. LOV KELCH PROTEIN2 and ZEITLUPE repress Arabidopsis photoperiodic flowering under non-inductive conditions, dependent on FLAVIN-BINDING KELCH REPEAT F-BOX1. *Plant J.* **2011**, *67*, 608–621. [CrossRef]
24. Hwang, D.Y.; Park, S.; Lee, S.; Lee, S.S.; Imaizumi, T.; Song, Y.H. GIGANTEA Regulates the Timing Stabilization of CONSTANS by Altering the Interaction between FKF1 and ZEITLUPE. *Mol. Cells* **2019**, *42*, 693–701. [CrossRef]
25. Yu, Y.T.; Portoles, S.; Ren, Y.; Sun, G.Y.; Wang, X.F.; Zhang, H.H.; Guo, S.G. The key clock component ZEITLUPE (ZTL) negatively regulates ABA signaling by degradation of CHLH in Arabidopsis. *Front. Plant Sci.* **2022**, *1*, 9959073. [CrossRef]
26. Jurca, M.; Sjoelander, J.; Ibanez, C.; Matrosova, A.; Johansson, M.; Kozarewa, I.; Takata, N.; Bako, L.; Webb, A.A.R.; Israelsson-Nordstroem, M.; et al. ZEITLUPE Promotes ABA-Induced Stomatal Closure in Arabidopsis and Populus. *Front. Plant Sci.* **2022**, *13*, 829121. [CrossRef]
27. Chor, B.; Hendy, M.D.; Holland, B.R.; Penny, D. Multiple Maxima of Likelihood in Phylogenetic Trees: An Analytic Approach. *Mol. Biol. Evol.* **2000**, *17*, 1529–1541. [CrossRef]
28. Wang, X.N. Research on Phenology and Blossom Biology of Oil-Tea Camellia. Master's Thesis, Central South University of Forestry and Technology, Changsha, China, 2011.
29. Tai, Y.; Wei, C.; Yang, H.; Zhang, L.; Chen, Q.; Deng, W.; Wei, S.; Zhang, J.; Fang, C.; Ho, C.; et al. Transcriptomic and phytochemical analysis of the biosynthesis of characteristic constituents in tea (*Camellia sinensis*) compared with oil tea (*Camellia oleifera*). *BMC Plant Biol.* **2015**, *15*, 190. [CrossRef]
30. Wiktorek-Smagur, A.; Hnatuszko-Konka, K.; Kononowicz, A.K. Flower bud dipping or vacuum infiltration-two methods of Arabidopsis thaliana transformation. *Russ. J. Plant Physiol.* **2009**, *56*, 560–568. [CrossRef]
31. Chang, M.M.; Li, A.; Feissner, R.; Ahmad, T. RT-qPCR demonstrates light-dependent AtRBCS1A and AtRBCS3B mRNA expressions in Arabidopsis thaliana leaves. *Biochem. Mol. Biol. Educ.* **2016**, *44*, 405–411. [CrossRef]
32. Makuch, L. Yeast Two-Hybrid Screen. *Methods Enzymol.* **2014**, *539*, 31–51. [CrossRef]
33. Soellick, T.R.; Uhrig, J.F. Development of an optimized interaction-mating protocol for large-scale yeast two-hybrid analyses. *Genome Biol.* **2001**, *2*, research0052.0051. [CrossRef]
34. Baudry, A.; Ito, S.; Song, Y.H.; Strait, A.A.; Kiba, T.; Lu, S.; Henriques, R.; Pruneda-Paz, J.L.; Chua, N.H.; Tobin, E.M.; et al. F-Box Proteins FKF1 and LKP2 Act in Concert with ZEITLUPE to Control Arabidopsis Clock Progression. *Plant Cell* **2010**, *22*, 606–622. [CrossRef]
35. Zoltowski, B.D.; Imaizumi, T. Structure and Function of the ZTL/FKF1/LKP2 Group Proteins in Arabidopsis. *Enzymes* **2014**, *35*, 213–239. [CrossRef] [PubMed]
36. Zienkiewicz, A.; Smoliński, D.J.; Zienkiewicz, K.; Glazińska, P.; Wojciechowski, W.; Kopcewicz, J. Molecular and cytological characterization of ZTL in Ipomoea nil. *Biol. Plant* **2009**, *53*, 435–443. [CrossRef]
37. Xue, Z.G. Cloning and Functional Analysis of GmZTL3 and GmZTL4 in Soybean. Master's Thesis, Henan Agricultural University, Zhengzhou, China, 2011.
38. Yang, W.Q. Studies on the Functions of OsZTL1 and OsZTL2 in Rice. Ph.D. Thesis, Shenyang Agricultural University, Liaoning, China, 2019. [CrossRef]
39. Zhao, F. Functional Analysis of Soybean GmZTL Gene. Master's Thesis, Guizhou University, Guiyang, China, 2008.
40. Xue, Z.G.; Zhang, X.M.; Lei, C.F.; Chen, X.J.; Fu, Y.F. Molecular cloning and functional analysis of one ZEITLUPE homolog GmZT L3 in soybean. *Mol. Biol. Rep.* **2012**, *39*, 1411–1418. [CrossRef] [PubMed]
41. Niwa, Y.; Yamashino, T.; Mizuno, T. The circadian clock regulates the photoperiodic response of hypocotyl elongation through a coincidence mechanism in Arabidopsis thaliana. *Plant Cell Physiol.* **2009**, *50*, 838–854. [CrossRef] [PubMed]
42. Fujiwara, S. Novel blue light receptors with an F-box: Their direct control of the circadian clock and the flowering timing in Arabidopsis. *Plant Biotechnol.* **2008**, *25*, 123–129. [CrossRef]
43. Song, Y.H.; Estrada, D.A.; Johnson, R.S.; Kim, S.K.; Lee, S.Y.; MacCoss, M.J.; Imaizumi, T. Distinct roles of FKF1, Gigantea, and Zeitlupe proteins in the regulat ion of Constans stability in Arabidopsis photoperiodic flowering. *Proc. Natl. Acad. Sci. USA* **2014**, *111*, 17672–17677. [CrossRef]
44. Lockhart, J. Membrane bound: C2-domain abscisic acid-related proteins help abscisic acid receptors get where they need to go. *Plant Cell* **2014**, *26*, 4566. [CrossRef]
45. Xiong, T.; Tan, Q.; Li, S.; Mazars, C.; Galaud, J.P.; Zhu, X. Interactions between calcium and ABA signaling pathways in the regulat ion of fruit ripening. *J. Plant Physiol.* **2021**, *256*, 153309. [CrossRef] [PubMed]

46. Diaz, M.; Sanchez-Barrena, M.J.; Gonzalez-Rubio, J.M.; Rodriguez, L.; Fernandez, D.; Antoni, R.; Yunta, C.; Belda-Palazon, B.; Gonzalez-Guzman, M.; Peirats-Llobet, M.; et al. Calcium-dependent oligomerization of CAR proteins at cell membrane mod ulates ABA signaling. *Proc. Natl. Acad. Sci. USA* **2016**, *113*, E396–E405. [CrossRef] [PubMed]
47. Sengupta, S.; Rajasekaran, K.; Baisakh, N. Natural and targeted isovariants of the rice actin depolymerizing factor 2 can alter its functional and regulatory binding properties. *Biochem. Biophys. Res. Commun.* **2018**, *503*, 1516–1523. [CrossRef] [PubMed]
48. Wang, L.; Qiu, T.Q.; Yue, J.R.; Guo, N.N.; He, Y.J.; Han, X.P.; Wang, Q.Y.; Jia, P.F.; Wang, H.D.; Li, M.Z.; et al. Arabidopsis ADF1 is Regulated by MYB73 and is Involved in Response to Salt Stress Affecting Actin Filament Organization. *Plant Cell Physiol.* **2021**, *62*, 1387–1395. [CrossRef]
49. Qian, D.; Zhang, Z.; He, J.X.; Zhang, P.; Ou, X.B.; Li, T.; Niu, L.P.; Nan, Q.; Niu, Y.; He, W.L.; et al. Arabidopsis ADF5 promotes stomatal closure by regulating actin cytoskeleton remodeling in response to ABA and drought stress. *J. Exp. Bot.* **2019**, *70*, 435–446. [CrossRef]
50. Huang, S.J.; Qu, X.L.; Zhang, R.H. Plant villins: Versatile actin regulatory proteins. *J. Integr. Plant Biol.* **2015**, *57*, 40–49. [CrossRef]
51. Alcântara, P.; Martim, L.; Silva, C.; Dietrich, S.; Buckeridge, M. Purification of a β-galactosidase from cotyledons of *Hymenaea courbaril* L. (Leguminosae). Enzyme properties and biological function. *Plant Physiol. Biochem.* **2006**, *44*, 619–627. [CrossRef]
52. McAllister, C.H.; Wolansky, M.; Good, A.G. The impact on nitrogen-efficient phenotypes when aspartate aminotransferase is expressed tissue-specifically in Brassica napus. *New Negat. Plant Sci.* **2016**, *3–4*, 1–9. [CrossRef]
53. Garchery, C.; Gest, N.; Do, P.T.; Alhagdow, M.; Baldet, P.; Menard, G.; Rothan, C.; Massot, C.; Gautier, H.; Aarrouf, J.; et al. A diminution in ascorbate oxidase activity affects carbon allocation and improves yield in tomato under water deficit. *Plant Cell Environ.* **2013**, *36*, 159–175. [CrossRef]
54. Stevens, R.; Truffault, V.; Baldet, P.; Gautier, H. Ascorbate Oxidase in Plant Growth, Development, and Stress Tolerance. In *Ascorbic Acid in Plant Growth, Development and Stress Tolerance*; Hossain, M.A., Munné-Bosch, S., Burritt, D.J., Diaz-Vivancos, P., Fujita, M., Lorence, A., Eds.; Springer International Publishing: Cham, Switzerland, 2017; pp. 273–295.

Disclaimer/Publisher's Note: The statements, opinions and data contained in all publications are solely those of the individual author(s) and contributor(s) and not of MDPI and/or the editor(s). MDPI and/or the editor(s) disclaim responsibility for any injury to people or property resulting from any ideas, methods, instructions or products referred to in the content.